Muon's Behaviors under Bremsstrahlung with both the LPM effect and the Ter-Mikaelian effect and Direct Pair Production with the LPM effect

S. Polityko¹, N. Takahashi², M. Kato³, Y. Yamada⁴ and A. Misaki⁵

¹Irkutsk State University, Irkutsk, 664003 Russia

²Facutly of Science and Technology, Hirosaki University,

Hirosaki 036-8561 Japan

³Kyowa Interface Science Co.Ltd., Asaka, 351-0033 Japan

⁴Hitachi Goverment and Public Cooperation System

Engineering Ltd., Koto-ku, Tokyo, 136-8633 Japan

⁵National Graduate Institute for Policy Studies,

2-2 Wakamatsu-cho, Shinjyuko-ku, 162-8677

and Institute for Policy Science, Saitama University,

Urawa 338-8570 Japan

November 1999

Abstract

Differential and integral cross sections of the muon are calculated in the materials: water, standard rock, iron and lead with and without the LPM effect. The corresponding cross sections are also calculated with dielectric supression effect (Ter-Mikaelian effect), in addition to the LPM effect. In our calculations the LPM effect for muon is provided to be effective from 10^{14} eV to 10^{20} eV depending on materials in the bremsstrahlung process, while it is provided to be completely negligible in the direct pair production process up to 10^{22} eV even for lead.

As for the dielectric suppression effect it is only effective between 10^{12} eV and 10^{20} eV in the case with the LPM effect, while it is effective above 10^{12} eV in the case without LPM effect. To demonstrate the importance of the LPM effect in the bremsstrahlung process, depth intensity relation of muon, energy spectrum, range distribution and survival probability are calculated taking into account bremsstrahlung spectrum.

1 Introduction

In the early 1950's, Landau, Pomeranchuk and Migdal realized that because of the low longitudinal momentum transfer between the nucleus and the fast particle, bremsstrahlung is not instantaneous, but occurs over a finite formation zone. During this time, external influences can perturb the fast particle and suppress the photon emission. When this happens, the usual Bethe-Heitler formula fails. Initially, Landau and Pomeranchuk studied suppression by multiple scattering with semiclassical argument [1]. Later, Migdal presented a fully quantum treatment[2]. Now this phenomenon is well known as the LPM effect. Cosmic ray physicists have been interested in the LPM effect which becomes effective at extremely high energies. Besides the LPM effect is expected to change drastically the structure of the electromagnetic cascade showers at extremely high energies, the structures of which are closely related to their physical interpretation. Up to now, the experimental proofs of the LPM effect have been tried by many investigators in both cosmic rays [3] and accelerators [4],[5].

Recently, the existence of the LPM effect has been finally confirmed by the SLAC electron accelerator [6] and the longitudinal effect [7] has been also reconfirmed [8]. Electromagnetic cascade shower with the

LPM effect is called the LPM shower, while the LPM effect, namely that at not-extremely high energies is called the BH (Bethe-Heitler) shower. The LPM shower has two distinguished characteristics over the BH shower: a) The average behaviors of the LPM shower are quite different from those of the BH shower [9] and b) The individual behaviors of the LPM shower are quite average behaviors of the LPM showers [10].

From the first characteristics of the LPM shower, we could easily understand that the size of the experimental apparatus for extremely high energy phenomena required should be much larger than that in usually imagined, while from the second characteristics of the LPM shower we understand that we should create a new method to analyze extremely high energy phenomena which could not be analyzed by the average theory.

Up to now, we have discussed the characteristics of the LPM effect on the electrons and photons. On the other hand, the LPM effect due to muon is also important for extremely high energy phenomena., particularly, for studies on extremely high energy neutrino astrophysics which are quite an uncultivated field. Now, there are two test pilot experiments for high energy neutrino astrophysics experiment in Baikal [11] and in Antarctic [12]. In future, we expect to construct the gigantic extremely high energy neutrino astrophysics detector, where the principle of the construction for the apparatus should be different from that of extremely high energy neutrino astrophysics due to the presence of the LPM effect. For the moment, it is more plausible that extremely high energy neutrino could be detected as extremely high energy muon from the neutrino interaction. In this energy region, the fluctuations are expected to play a decisivly important role for the energy determination of muon neutrino at extremely high energy (over $10^{15}eV$). The fluctuations in this energy region come from (a) the LPM effect due to the muon and (b) the LPM effect due to electron (electromagnetic cascade shower).

In this paper, we would like to discuss the case (a) which has never been discussed before. Without exact consideration of the LPM effect in both muon and electron (photon) we could not determine the energy of the muon at extremely high energies.

2 Theory: derivation of cross-section

At first we remind here the semiclassical picture of LPM. The radiation of a relativistic particle in matter develops in a large region of space along its momentum. The characteristic size of this region can be easily estimated. When the muon is of a sufficiently high momentum, q the longitudinal momentum carried by the virtual photon, becomes very small,

$$q = p_{\mu} - p'_{\mu} - k = \sqrt{E_{\mu}^2 - m_{\mu}^2} - \sqrt{E_{\mu}^{\prime 2} - m_{\mu}^2} - E_{\gamma}, \tag{1}$$

where $p_{\mu}, p'_{\mu}, E_{\mu}$ and E'_{μ} are the muon momentum and energy before and after the interaction, respectively, and E_{γ} is the photon energy and γ is Lorentz factor. For high energy muons this simplifies to

$$q \sim \frac{m_{\mu}^2 E_{\gamma}}{2E_{\mu}(E_{\mu} - E_{\gamma})} = \frac{m_{\mu}}{2\gamma} \frac{u}{1 - u},$$
 (2)

where $u = E_{\gamma}/E_{\mu}$ is the fractional energy of the radiated photon. This momentum transfer can be very small. Then, by the uncertainty principle, the virtual photon exchanges the distance l_c

$$l_c \sim \frac{\hbar}{q} = \frac{2E_\mu^2}{m_\mu^2 E_\gamma} \tag{3}$$

For example, for a 100 TeV muon emitting a 1 GeV photon, q is $0.56 \cdot 10^{-3} eV/c$ and the coherence length is $3.5 \cdot 10^{-2}$ cm.

The coherence length can also be interpreted as the length in which stripping of a photon from the muon which radiates it occurs.

The LPM effect appears when one considers that the muon must be undisturbed while it traverses this distance. One factor that can disturb the muon and disrupt the bremsstrahlung is multiple Coulomb scattering. Semiclassically, if the muon multiple scatters by an angle θ_s , greater than the angle made

by the bremsstrahlung photon, $\theta_{br} \sim 1/\gamma$, then the bremsstrahlung is suppressed. The average multiple scattering angle in a nuclear medium is

$$\langle \theta_s^2 \rangle = \left(\frac{E_s}{E}\right)^2 \frac{l}{X_0},$$
 (4)

where $E_s = \sqrt{4\pi/\alpha}m = 21$ MeV is the characteristic energy, l is the scatter thickness, and X_0 is the radiation length. The LPM effect becomes important when θ_s is larger than θ_{br} . This occurs for

$$\left(\frac{E_s}{E}\right)\sqrt{\frac{l}{X_0}} > \frac{1}{\gamma}$$

If l_c is larger than the size of an atom, it is necessary to take into account the interaction of the incident muon not only with the nucleus of the atom but also with the atomic electrons. This interaction is taken into account as the screening effect in the Bethe-Heitler theory of bremsstrahlung. If l_c exceeds the average distance between the atoms of medium, then it is necessary to take into consideration the influence both of the atomic electrons and of many atoms on the particle radiation process.

The coherence length increases with decrease of the frequency of the radiated photon, and for sufficiently small E_{γ} it can reach macroscopic dimensions. Therefore, the LPM effect modifies the soft part of bremsstrahlung spectrum. For the low energy photon, the photon spectrum is proportional to $E_{\gamma}^{-1/2}$, in contrast to the $1/E_{\gamma}$ Bethe-Heitler spectrum.

An analogous effect occurs for pair creation by a high energy photon. In pair creation, the LPM energy threshold is determined by the lepton with the low energy. Because of this, the pair creation suppression begins at more higher energies than bremsstrahlung suppression.

At low bremsstrahlung photon energies dielectric suppression effect occurs (also known as the longitudinal density effect). This influence can be taken into account by introducing dielectric permeability $\varepsilon(E_{\gamma})$. Ter-Mikaelian showed, that in the case of soft photons the discount of dielectric permeability also leads to decrease of bremsstrahlung probability [13]. Recently these effects have been observed experimentally [8]. These phenomena are important in the development of electromagnetic shower accompaning the high energy muon. Thus for the modelling of electromagnetic showers it is necessary to use the probabilities, including LPM effect and the longitudinal density effect. Earlier the discount of LPM effect for bremsstrahlung and direct pair production by muon has been carried out in [14].

2.1 Bremsstrahlung of muon in a medium

The appropriate method to consider radiative effects in media is the quasiclassic approach of considering the processes of bremsstrahlung and direct pair production [15],[16]. Let $k = (E_{\gamma}, \vec{k}_{\gamma})$ - be the 4-momentum of bremsstrahlung photons.

The probability of radiation of a photon by the high energy muon per a time unit averaged in initial muon polarization and summed in final particles polarization has the form

$$dW = \frac{\alpha}{(2\pi)^2} \frac{d^3 k_{\gamma}}{E_{\gamma}} \frac{1}{2T} Re \int_{-T}^{T} dt \int_{0}^{\infty} d\tau \exp(-i\tilde{k}(x(t+\tau) - x(t)) \mathcal{L}(\vec{p}(t+\tau), \vec{p}(t))), \tag{5}$$

where $\mathcal{L}(\vec{p}(t+\tau), \vec{p}(t))$ - is a square of matrix elements of muon photon radiation,

$$\tilde{k}_0 = E_\mu E_\gamma / (E_\mu - E_\gamma) - (E_\gamma^2 - \vec{k}_\gamma^2) / 2(E_\mu - E_\gamma), \, \vec{\tilde{k}} = E_\mu \vec{k}_\gamma / (E_\mu - E_\gamma)$$
(6)

This formula determines the radiation probability on the set trajectory and must be averaged in all possible trajectories. Averaging is realized due to the distribution function which satisfies to the standard kinetic equation

$$\partial F/\partial t + \vec{v}\partial F/\partial \vec{r} = nv \int \sigma(\vec{v}, \vec{v}') [F(\vec{r}, \vec{v}, t) - F(\vec{r}, \vec{v}', t)] d\vec{v}'$$
(7)

with the initial condition

$$F(\vec{r}, \vec{r'}, 0, \vec{v}, \vec{v'}) = \delta(\vec{r} - \vec{r'})\delta(\vec{v} - \vec{v'})$$

Here $\sigma(\vec{v}, \vec{v}')$ is the scattering cross-section in Couloumb field with the account of full screening

$$\sigma(\vec{v}, \vec{v}') = \frac{4E_{\mu}^2 Z^2 \alpha^2}{[(\vec{p}' - \vec{p})^2 + \chi^2]},\tag{8}$$

where χ - is the screening constant in Thomas-Fermi approximation

In small angle approximation after integration by coordinates the kinetic equation transforms into Fokker-Planck equation

$$\partial F/\partial \tau + i(a + b\theta^2/2)F = q\Delta F \tag{9}$$

where

$$q = \frac{2\pi n Z^2 \alpha^2}{E_{\mu}^2} \ln\left(\frac{\theta_2}{\theta_1}\right), \qquad a = \frac{\omega_0^2}{2E_{\gamma}} + \frac{m_{\mu}^2 E_{\gamma}}{2E_{\mu}(E_{\mu} - E_{\gamma})}, \qquad b = \frac{E_{\gamma} E_{\mu}}{E_{\mu} - E_{\gamma}}, \tag{10}$$

 θ_1 and θ_2 are minimal and maximal angles of scattering in bremsstrahlung formation process, n is the density of scattering centers. The details to solve Fokker-Planck equation can be found in [15]. Here we show only the final result

$$F(\theta, \theta', \tau) = \exp(\alpha(\tau)\theta'^2 + \beta(\tau)\theta\theta' + \gamma(\tau)), \tag{11}$$

where

$$\alpha(\tau) = -\sqrt{ib/8q} \coth(\sqrt{2ibq}\tau),$$

$$\beta(\tau) = \sqrt{ib/2q} \sinh^{-1}(\sqrt{2ibq}\tau),$$

$$\gamma(\tau) = -ia\tau - \ln(\sinh(\sqrt{2ibq}\tau)) + \theta^2 \alpha(\tau) + \ln(\sqrt{ib/8q}).$$

For $\mathcal{L}(\vec{p}', \vec{p})$ in small angle approximation we have

$$\mathcal{L}(\vec{p}', \vec{p}) = R_1 + R_2 \theta \theta', \tag{12}$$

where

$$R_1 = \frac{m_{\mu}^2 E_{\gamma}^2}{E_{\mu}^2 (E_{\mu} - E_{\gamma})^2}, \qquad R_2 = \frac{E_{\mu}^2 + (E_{\mu} - E_{\gamma})^2}{(E_{\mu} - E_{\gamma})^2}.$$

As a result the quasiclassic approximation calculation gives the probability of bremsstrahlung in the following form:

$$dW = \frac{\alpha}{2\pi} q \frac{E_{\gamma} dE_{\gamma}}{b} \left[\frac{b}{3a^2} R_1 G(s) + \frac{4}{3a} R_2 \Phi(s) \right]$$
(13)

Here $s = a/4\sqrt{bq}$, G(s) and $\Phi(s)$ are the famous Migdals functions.

The indefinity in $\ln(\theta_2/\theta_1)$ is the result of transition to Fokker-Planck equation in approximation of small angles.

The argument of logarithm contains the indefinite numerical factor. This factor can be defined in the limited case $(s \gg 1)^{-1}$.

In this case formula (5) goes over to usual bremsstrahlung formula Bethe-Heitler. The comparison of the limited expression with the formula of Petrukhin and Shestakov [17],[19] gives us

$$\ln\left(\frac{\theta_2}{\theta_1}\right) = \xi(s)L\tag{14}$$

where L from [17] is

$$L = \ln\left(\frac{126m_{\mu}Z^{-2/3}/m_e}{1 + 189\sqrt{e}\delta Z^{-1/3}/m_e}\right), \quad \text{if} \quad Z > 10, \tag{15}$$

¹Semiclassically, this condition corresponds to $\theta_{br} \gg \theta_s$

$$L = \ln\left(\frac{189m_{\mu}Z^{-1/3}/m_e}{1 + 189\sqrt{e}\delta Z^{-1/3}/m_e}\right), \quad \text{if} \quad Z \le 10$$
 (16)

Here $\delta = m_{\mu}^2 u/2E_{\mu}(1-u)$ is the minimum momentum transfer to the nucleus and e = 2.718. (for the electron $L = \ln(190Z^{-1/3})$).

Therefore we can define the value s:

$$s = \frac{1}{8} \left(\frac{1}{2\pi} \frac{1}{\gamma_{\mu}} \frac{u}{(1-u)} \frac{m_{\mu}^{3}}{nZ^{2}\alpha^{2}L} \right)^{1/2}, \quad u = \frac{E_{\gamma}}{E_{\mu}}, \qquad \gamma_{\mu} = \frac{E_{\mu}}{m_{\mu}}. \tag{17}$$

Phenomenological factor $\xi(s)$, according to Migdal, equals:

$$\xi(s) = \begin{cases} 1, & \text{if } s > 1\\ 1 + \ln(s) / \ln(s_1), & \text{if } s_1 < s < 1\\ 2, & \text{if } s < s_1 \end{cases}$$
(18)

where the value s_1 :

$$s_1^{1/2} = \begin{cases} m_e Z^{1/3} / 189 m_\mu, & \text{if } Z < 10\\ m_e Z^{2/3} / 126 m_\mu, & \text{if } Z > 10 \end{cases}$$
 (19)

The obtained result has the logarithmic accuracy and does not contain Coulomb corrections. The use of the more accurate formula [20] as a limit case is difficult because it has not only non-logarithmic terms but also corrections proportional to Z and 1/Z. The accuracy of Migdal's calculations is discussed at first in [5]. Recently in [21] the calculation with more accuracy has been performed for electron LPM effect. These calculations showed that the Migdal calculations have the 10-15 % accuracy.

2.2 The longitudinal effect

Now we consider the longitudinal effect, namely, the influence of media polarization. We can rewrite the expression of a from formulae (10):

$$a = \frac{\omega_0^2}{2E_{\gamma}} + \frac{m_{\mu}^2 E_{\gamma}}{2E_{\mu}(E_{\mu} - E_{\gamma})} =$$

$$= \frac{m_{\mu}^2 E_{\gamma}}{2E_{\mu}(E_{\mu} - E_{\gamma})} \left[1 + \frac{\omega_0^2 E_{\mu}(E_{\mu} - E_{\gamma})}{E_{\gamma}^2 m_{\mu}^2} \right]$$

$$\approx \frac{m_{\mu}^2 E_{\gamma}}{2E_{\mu}(E_{\mu} - E_{\gamma})} \cdot \left[1 + \frac{\omega_0^2}{u^2 m_{\mu}^2} \right].$$
(20)

Therefore we have the additional factor d_{μ} :

$$d_{\mu} = 1 + \frac{\omega_0^2}{u^2 m_{\mu}^2} \tag{21}$$

This factor changes the expression for bremsstrahlung cross-section (the function $\Phi(s) \to \Phi(s)/d_{\mu}$, $G(s) \to G(s)/d_{\mu}^2$ and the value of $s \to d_{\mu} \cdot s$).

Finally the cross-section is

$$\frac{d\sigma}{du} = \alpha^3 \left(\frac{2Z}{m_\mu}\right)^2 \frac{\xi(s)L}{u} \left(\frac{1}{3} \frac{u^2 G(s)}{d_\mu^2} + \left(\frac{4}{3} - \frac{4}{3}u + \frac{2}{3}u^2\right) \frac{\Phi(s)}{d_\mu}\right),\tag{22}$$

parameter s can be written as

$$s = d_{\mu} \cdot \frac{1}{8} \left(\frac{E_{LPM}}{E_{\mu}} \frac{u}{1 - u} \right)^{1/2}, \quad E_{LPM} = \frac{m_{\mu}^4}{2\pi n Z^2 \alpha^2 L}. \tag{23}$$

We illustrate these both phenomena by some numerical calculations. Parameters of some media are collected in Table 1.

The condition s < 1 gives us a simple relation for the energy of bremsstrahlung photon, where LPM effect is important:

$$E_{\gamma} < \frac{64E_{\mu}^2}{E_{LPM}}$$

The dielectric suppression (effect longitudinal density) is essential at the condition $d_{\mu} > 2$:

$$E_{\gamma} < \frac{E_{\mu}\omega_0}{E_{LPM}}.$$

Thus, for example, the corresponding values E_{γ} in water for muon energy $E_{\mu} = 10^{15} \ eV$ equals $E_{\gamma} < 25$ MeV (LPM) and $E_{\gamma} < 200$ MeV (effect of longitudinal density)

2.3 Direct electron pair production by muon in a medium

For the process of direct pair production (DPP) the double differential probability in the total energy pair and in the energy of one component (electron or positron) can be obtained, following the paper of Ternovskii [22]. The process DPP contains the integration on the virtual photon momentum, therefore the answer is expressed through the integral on the Migdal functions. The probability of DPP has the following form:

$$dW(E_{\mu}, E_{p}, E_{+}) = \frac{2}{3\pi} n r_{e}^{2} Z^{2} \alpha^{2} \ln\left(\frac{\theta_{2}}{\theta_{1}}\right) \frac{dE_{p} dE_{+}}{E_{p}^{2}} \left[\left\{ 1 + \left(1 - \frac{E_{p}}{E_{\mu}}\right)^{2} \right\} \left\{ A(s, x) + 2\left(\frac{E_{+}^{2}}{E_{p}^{2}} + \left(1 - \frac{E_{+}}{E_{p}}\right)^{2}\right) B(s, x) \right\} + \frac{E_{p}^{2}}{E_{\mu}^{2}} \left\{ C(s, x) + 2\left(\frac{E_{+}^{2}}{E_{p}^{2}} + \left(1 - \frac{E_{+}}{E_{p}}\right)^{2}\right) D(s, x) \right\} + 8\frac{E_{+}}{E_{p}} \left(1 - \frac{E_{+}}{E_{p}}\right) \left(1 - \frac{E_{p}}{E_{\mu}}\right) E(s, x) \right], (24)$$

where $E_p = E_+ + E_-, E_+$ and E_- are the energies of component pair.

Let us introduce the following variables:

$$\rho = \frac{E_{+} - E_{-}}{E_{+} + E_{-}}, \quad v = \frac{E_{+} + E_{-}}{E_{\mu}} = \frac{E_{p}}{E_{\mu}}.$$
 (25)

Thus, we have the following expression for the double differential cross-section:

$$\frac{d^2\sigma}{d\rho dv} = \frac{2}{3\pi} r_e^2 Z^2 \alpha^2 \ln\left(\frac{\theta_2}{\theta_1}\right) \frac{1-v}{v} \cdot$$

$$((1+\beta)(A(s,x) + (1+\rho^2)B(s,x)) + \beta(C(s,x) + (1+\rho^2)D(s,x)) + (1-\rho^2)E(s,x))$$
(26)

Here we calculated the Jacobian

$$dE_{+}dE_{p} \to E_{\mu}^{2} \frac{vdvd\rho}{2} \tag{27}$$

and denote

$$\beta = \frac{v^2}{2(1-v)}, \quad x = \frac{m_{\mu}^2}{m_e^2} \frac{v^2(1-\rho^2)}{4(1-v)},\tag{28}$$

$$s = \frac{1}{4} \left(\frac{E_{LPM}}{E_{\mu}} \frac{1}{v(1 - \rho^2)} \right)^{1/2}, \quad E_{LPM} = \frac{m_{\mu}^4}{2\pi n Z^2 \alpha^2 L}. \tag{29}$$

The integration limits are:

$$\frac{2m_e}{E_\mu} < v < 1 - \frac{3\sqrt{e}m_\mu}{4E_\mu}Z^{1/3} \tag{30}$$

$$0 < |\rho| < \left(1 - \frac{6m_{\mu}^2}{E_{\mu}^2(1 - v)}\right) \sqrt{1 - 2m_e/E_{\mu}v} \tag{31}$$

The expressions for coefficients A(s,x), B(s,x), C(s,x), D(s,x) and E(s,x) are given in Appendix A ². The argument of logarithm contains the indefinite numerical factor. This factor can be defined in the limited case $(s \gg 1)$. In this case formula (7) goes over to usual formula of cross-section direct pair production. The comparison of the limited expression with formula of Petruchin and Kokoulin [17],[18] gives us

$$ln(\frac{\theta_2}{\theta_1}) = L_e = L.$$
(32)

where L_e from [17]:

$$L_e \approx \ln(189Z^{-1/3}\sqrt{(1+x)(1+Y_e)})$$
 (33)

Here

$$Y_e = \frac{5 - \rho^2 + 4\beta(1 + \rho^2)}{2(1 + 3\beta)\ln(3 + 1/x) - \rho^2 - 2\beta(2 - \rho^2)}$$
(34)

For numerical estimations we can take out the minimal value $(1+x)(1+Y_e) \sim 3.25$, therefore $L = \ln(614Z^{-1/3})$. The values of E_{LPM} for water, standard rock and lead are listed in Table 2.

The role of LPM is essential for the process of DPP at

The values of E_{LPM} for bremsstrahlung and for DPP differ from each other only by the quantity L. This logarithm is the slowly changeable value depending on the medium properties.

The energy E_{μ} is larger for the process of DPP, since the momentum of virtual photons $p_{\gamma^*}^2 \geq 4m_e^2$ for the production of e^+e^- pairs. The LPM is more expressed in the symmetrical case, i.e. $\rho = 0$ or $E_+ \sim E_-$ for the direct pair production.

The probability of production $\mu^+\mu^-$ is

$$dW_{\mu^{+}\mu^{-}} \approx \frac{m_{e}^{2}}{m_{\mu}^{2}} dW_{e^{+}e^{-}} \tag{35}$$

therefore it should not be probably taken into account.

3 Numerical calculation of the cross-section

3.1 Bremsstrahlung process

 $^{^2}$ The error from using these expressions gives us 0.7 % accuracy at $E_{\mu}<10^{22}~eV$ and is less than 15 % accuracy at $E_{\mu}>10^{24}eV$

3.1.1 The longitudinal density effect (Ter-Mikaelian effect)

The longitudinal density effect (the LD effect) exists irrespectively of the absence or presence of the LPM effect in the bremsstrahlung process. Therefore, we evaluate the contribution from the LD effect to the differential cross section. In Figures 1 to 4, we calculate the differential cross sections for water, standard rock, iron and lead, respectively, where BH denotes "without the LPM effect". In these figures, the differential cross sections of BH, (BH and LD), LPM and (LPM+BH) are given. It is easily understood that the LD effect suppresses much lower energy photon, compared to the LPM effect. And it is also understood that the LD effect is more effective in higher density materials. Further it should be noted the following: the fact that BH+LD coincide with LPM+LD at smaller u in from Figs.1 to 4 meaning that the LD effect is only effective in the region at smaller u. However the LD effect is not so effective compared to the LPM effect, as in the same situation in the case of electron 3

In order to examine the contribution from the LD effect over muon's propagation, we calculate the corresponding integral cross section (the total cross section) due to the LD effect in Figures 5 and 6.

In Figure 5, we give the ratio of (BH and LD) to BH from $10^9 \ eV$ to $10^{24} \ eV$. In the calculation for total cross sections throughout present work, the lower bound for integration is $10^6 \ eV$. From the figure we could realize that the LD effect is not effective up to $10^{12} \ eV$. The LD effect begins to be effective around $10^{12} \ eV$ and makes the integral cross sections decrease to 60 % or more at $10^{24} \ eV$ in the absence of the LPM effect. However, we notice that not a small apparent decrease of the ratio exclusively comes from infra-red divergence due to the Bethe-Heitler's cross section which never influences over the real behavior of higher energy muon and besides the LD effect is negligible compared to the LPM effect at such higher energies , which are shown in Figure 6. Comparing Figure 5 with Figure 6, it is easy to understand that (1) the LD effect is only effective and the LPM effect is never effective up to around $10^{14} \ eV$, (2) the competition occurs between the LD effect and the LPM effect from $10^{14} \ eV$ to $10^{20} \ eV$, and (3) the LD effect is completely negligible at the energies more than $10^{20} \ eV$.

3.1.2 The LPM effect

From Figures 1 to 4, we understand that the LPM effect is more effective in higher density materials and becomes strong at more higher primary energy of muon. The radiated photon at lower energies is proportional to $\sim 1/\sqrt{E_{\gamma}}$, while that due to BH is proportional to $\sim 1/E_{\gamma}$, which is essentially the same as in the case of an electron.

In Figures 7 to 10, we give mean free paths due to the combination of different effects in water, standard rock, iron and lead, respectively. The mean free path of an electron due to the LPM effect increases as primary energy of muon increases and as the density of material is higher. Roughly speaking, elongations of the mean free paths are 20, 30, 70, 120 times as large as compared to the BH case in water, standard rock, iron and lead for the primary energy muon of 10^{24} eV, respectively. The mean free paths of muons with LPM effect are given in Figure 11, while those of the muon with both LPM and LD effects in Figure 12. Comparison of Figure 11 and Figure 12 shows that the mean free path of muon with both LPM effect and the LD effect increases by about fifty percent over 10^{12} eV and 10^{20} eV, which depends on the materials, due to the existence of the LD effect compared to the LPM effect only.

3.2 Direct electron-positron pair production process

As shown in the Appendix B, the LPM effect in the direct electron pair production process could be completely negligible up to 10^{24} eV even for lead. Therefore, we calculate the cross sections without the LPM effect only. In Figures 13-1 and 13-2, we give the virtual photon energy spectrum for primary energies of 10^{16} eV and 10^{24} eV for the materials of lead, iron, standard rock and water, respectively. After the integration by the energies of virtual photon, we obtain total cross sections due to the direct electron pair productions. In Figure 14, we give the total cross sections for lead, iron, standard rock and

³See subsequent paper

water. In Figure 15, we give the mean free paths of direct pair electrons for the same materials as in Figure 14.

4 Effective energy loss

Here let us define the effective energy loss of muon in the bremsstrahlung process[23] by examining the influence over "effective energy loss" to primary energy of muon.

$$\eta(E_{\mu}) = E_{\mu} \frac{N}{A} \int_{u_{min}}^{u_{max}} du \cdot u \cdot \frac{d}{du} \sigma_{LPM(BH)}(u, E_{\mu}), \tag{36}$$

where $\frac{d}{du}\sigma_{LPM(BH)}(u,E_{\mu})$ are the differential cross sections with and without LPM effect. Here, we take $u_{min}=10^6~eV$ and $u_{max}=1-m_{\mu}c^2/E_{\mu}$.

In the effective energy loss by muon, the influence of the longitudinal density effect could be completely neglected over $10^9 \ eV$ to $10^{24} \ eV$ in both the BH and the LPM cases.

In Figures 16-1 and 16-2 the effective energy loss due to bremsstrahlung process are given in both cases with and without the LPM effect in water and iron, and standard rock and lead, respectively. To clear the LPM effect on the effective energy loss, we give the ratio of effective energy loss with the LPM effect over that without the LPM effect in the following.

$$r(E_{\mu}) = \frac{\int_{u_{min}}^{u_{max}} du \cdot u \cdot \frac{d}{du} \sigma_{LPM}(u, E_{\mu})}{\int_{u_{min}}^{u_{max}} du \cdot u \cdot \frac{d}{du} \sigma_{BH}(u, E_{\mu})}$$
(37)

In Figure 17, the ratio calculated in (36) is given. It is shown in the figure that the LPM effect becomes effective over $10^{20} \ eV$, depending on the materials.

Also let us define the average energy transfer to the virtual photon due to direct pair electron production process in the following way.

$$\xi(E_{\mu}) = E_{\mu} \frac{N}{A} \int_{v_{min}}^{v_{max}} dv \int_{\rho_{min}}^{\rho_{max}} v \cdot \frac{d^2 \sigma}{d\rho dv} (v, E_{\mu}) d\rho, \tag{38}$$

where $\frac{d^2\sigma}{d\rho dv}(v, E_{\mu})d\rho$ is a double differential cross section for ρ and v in the direct pair production. Here the lower and upper bounds for integration are defined in (30), (31). The calculated results are given in Figure 18. As the LPM effect could be neglected completely in the direct electron production process shown in the previous section, the numerical results of (37) are given in the BH cases only.

5 Depth intensity relation of muons at extremely high energies

Studies on the depth intensity relation of muon at deeper depth in both water and rock are indispensable for elucidation of physics related to an extremely high energy muon. Depth intensity relation of muon is determined by the processes of bremsstrahlung, direct pair production, nuclear interaction and ionization loss. For the studies on the depth intensity relation of muon at extremely high energies, examination of the fluctuation effect from the bremsstrahlung process should be carefully made, because it is a strong source of the fluctuation. The following calculations are made to examine a fluctuation effect from bremsstrahlung. To obtain physically meaningful results at extremely high energies in the calculation on the depth intensity relation of muon one should consider not only bremsstrahlung but also the direct electron-positron pair production, nuclear interaction and ionization loss down to lower energies, for example at 1 GeV.

To examine the degree of the fluctuation from bremsstrahlung process at extremely high energies, we calculate the depth intensity relation of muons, taking into account the bremsstrahlung process only and keeping E_{prim}/E_{cut} to be 1000, where E_{prim} denotes the primary energy of the muon and E_{cut} denotes cut off energy of muon in the calculation and the related quantities.

In Figures 19-1 and 19-2, we give the average value of muon with and without the LPM effect in both standard rock and water. We give the average energy of muon with primary energies of $10^{24}eV$ and $10^{23}eV$. If the LPM effect becomes effective, the cross section decreases so that the average energy of muon becomes high. From Figures 19-1 and 19-2, we could understand that [1] the average energy of muon in standard rock is higher than that of water, [2] the LPM effect is more effective in $10^{24}eV$ than in $10^{23}eV$ in both cases with and without the LPM effect.

In Figure 20-1 and Figure 20-2, survival probabilities of muon are given in rock and water, respectively. Conditions given to the calculations are exactly the same as in Figures 19-2 and 21. If the LPM effect becomes essential, the cross section decreases so that survival probabilities become large. We could understand the following from both Figures . [1] Survival probability in the rock is larger than that in water. [2] The LPM effect is much more effective in $10^{24}eV$ than in $10^{23}eV$, [3] it gives much higher survival probabilities for every depth.

In both Figures 21-1 and 21-2, range fluctuation of muon are given in both standard rock and water. From both Figures, we could conclude the following: comparing the contrast of LPM 24-21 and LPM 23-20 in Figure 21-1 with those in Figure 21-2, the LPM effect is more essential in standard rock than that in water.

From Figure 21-2, Table 3 and Table 4, it is very interesting to note that the average values and their standard deviations are larger in water than in standard rock both with and without the LPM effect, as far as the fluctuation of range distributions are concerned.

In Figures 25-1,25-2 and 25-3, we show energy spectrum in water at the depths $10^6 g/cm^2$, $4 \cdot 10^6 g/cm^2$ and $8 \cdot 10^6 g/cm^2$ for primary energies of $10^{22} eV$, $10^{23} eV$ and $10^{24} eV$, in the case with the LPM effect and without the LPM effect (BH), respectively. From Figure 22-1, we could easily understand that the LPM effect is not essential almost over every depth and it shows little effect at depth $8 \cdot 10^6 g/cm^2$, because the chances to lose energy increase at larger depths than that at shallower depth so that the LPM effect begins to work. From Figure 23-2, we could understand that the LPM effect begins to become effective around $10^{23} eV$ From 23-3, we understand that the LPM effect becomes effective strongly, particularly at the depth $8 \cdot 10^9 g/cm^2$.

In Figures 23-1,23-2 and 23-3, we show the corresponding spectrum to Figures 22-1,22-2 and 22-3 in the standard rock. From the comparison of 23-1, 23-2, and 23-3 with Figures 22-1, 22-2 and 22-3, we could understand that the LPM effect is much effective in the standard rock than in water.

6 General Discussion

The practical purpose of the study of the muon with LPM effect for neutrino astrophysics is to offer theoretical means by which we could determine the energy of astronomical sources with extremely high energies. Such extremely high energy sources are expected to be found in the earth through the detection of the extremely high energy muon due to muon neutrino. The extremely high energy muon is suffered from strong fluctuation due to the LPM effect so that the determination of energy is so difficult. Therefore, the detailed studies on extremely high energy muon are requested for the purpose. Another purpose of the study on extremely high energy muon may be to clarify the mechanism of charm hadronproduction.

From the results thus obtained in too much simplified way, we try to conjecture results which correspond to the real experiments. To perform calculations of the depth intensity relation of muon which are really useful for the analysis of the experimental data at extremely high energy, if really exist, we must consider the direct electron pair production and nuclear interaction except the bremsstrahlung, and energy spectrum of muon at sea level and must make a calculation down to too much lower energy which corresponds to the real experiment compared to the present minimum energy $10^{20}eV$, say, $10^{9}eV$. Nevertheless, we could conjecture the following: the LPM effect becomes effective at extremely high energies and it appears strong at larger depth due to strong fluctuation effect, because characteristics of relation between primary muon with extremely high energy, say $10^{24}eV$ and that with still extremely high energy

cut off, say $10^{21}eV$, will be surely kept at the relation between primary muon with extremely high energy and that with too lower energy, say, 10^9eV which corresponds to the real experimental conditions. Further, over energy of $10^{15}eV$, the flux of prompt muon at sea level exceeds over that of conventional muon which is analyzed in the usual experimental data. Therefore, we could say that the LPM muon is appeared in the flux of prompt muon and the depth intensity relation of muon at extremely high energy is closely related to the analysis on the mechanism of the charm hadroproduction.

7 Acknowledgement

We would like to thank prof. F.F.Ternovskii for the useful discussion on the direct pair production. Also we thank prof. M.L.Ter-Mikaelian for the discussion about the longitudinal density effect.

Appendix A

A On calculation of Ternovskii functions

The integral representations of coefficients A(s,x), B(s,x), C(s,x), D(s,x), E(s,x) are given by

$$A(s,x) = \int_{1+x}^{\infty} \frac{(z-x-1)G(sz)dz}{z^2(z-1)^2}, \quad B(s,x) = \int_{1+x}^{\infty} \frac{(z-x-1)\Phi(sz)dz}{z(z-1)^2}, \quad (A-1)$$

$$C(s,x) = x \int_{1+x}^{\infty} \frac{G(sz)dz}{z^2(z-1)^2}, \quad D(s,x) = x \int_{1+x}^{\infty} \frac{\Phi(sz)dz}{z(z-1)^2}, \quad E(s,x) = \int_{1+x}^{\infty} \frac{G(sz)dz}{z^2}.$$

Now we write the approximation formulae for the functions A(s,x), B(s,x), C(s,x), D(s,x), E(s,x). The error from using these expressions gives us 0.7 % accuracy at $E_{\mu} < 10^{22}~eV$ and is less than 15 % accuracy at $E_{\mu} > 10^{24}~eV$. Here we used the following simple expression for the functions G(s) and $\Phi(s)$.

$$\Phi(s) \approx \frac{6s}{6s+1}, \quad G(s) \approx \frac{(6s)^2}{(6s)^2+1}$$

$$A(s,x) = \frac{18s^2}{36s^2+1} \left(1 + \frac{72s^2}{36s^2+1}x\right) \ln \frac{36s^2(1+x)^2+1}{36s^2x^2} - \frac{36s^2}{36s^2+1}$$

$$+ \frac{216s^3}{36s^2+1} \left(1 + \frac{36s^2-1}{36s^2+1}x\right) \left(Atan(6s(x+1)) - \frac{\pi}{2}\right)$$

$$B(s,x) = \frac{6s}{6s+1} \left(1 + \frac{6sx}{6s+1}\right) \ln \frac{6s(1+x)+1}{6sx} - \frac{6s}{6s+1}$$

$$C(s,x) = -\frac{(36s^2)^2x}{(36s^2+1)^2} \ln \frac{36s^2(1+x)^2+1}{36s^2x^2} + \frac{36s^2}{36s^2+1}$$

$$-\frac{216s^3(36s^2-1)}{(36s^2+1)^2} x \left(Atan(6s(x+1)) - \frac{\pi}{2}\right)$$

$$D(s,x) = \frac{6s}{6s+1} - \frac{36s^2x}{(6s+1)^2} \ln \frac{6s(1+x)+1}{6sx}$$

$$E(s,x) = 6s \left(\frac{\pi}{2} - Atan(6s(x+1))\right)$$

At $s \gg 1/(1+x)$ in complete agreement with the results of the theory neglecting effects of the medium we obtain

$$A(s,x) = (1+2x)\ln\left(1+\frac{1}{x}\right) - 2, \quad B(s,x) = (1+x)\ln\left(1+\frac{1}{x}\right) - 1,$$

$$C(s,x) = \frac{1+2x}{1+x} - 2x\ln\left(1+\frac{1}{x}\right), \qquad (A-3)$$

$$D(s,x) = 1 - x\ln\left(1+\frac{1}{x}\right), \quad E(s,x) = \frac{1}{1+x}.$$

And at $s \ll 1/(1+x)$ we obtain the expressions

$$A(s,x) = -36s^2 \ln(6sx), \quad B(s,x) = -6s \ln(6sx), \quad C(s,x) = 36s^2,$$

 $D(s,x) = 6s, \quad E(s,x) = 3\pi s.$ (A-4)

Appendix B

Here we show that the LPM effect could be completely negligible for the direct electron pair production process up to $10^{24}\ eV$ even for lead, by using the Ternovskii functions defined in the Appendix A. The double differential cross section for the direct electron pair production (DPP) process is given in (27). The LPM effect is included in the Ternovskii functions from A(s,x) to E(s,x) defined (A-1). The numerical orders of all the Ternovskii functions are the same. Therefore we consider the degree of the LPM effect in the function A(s,x) in the Appendix A, as an example.

A(s,x) is given as follows:

$$A(s,x) = \int_{1+x}^{\infty} \frac{(z-x-1)G(sz)dz}{z^2(z-1)^2}$$
 (B-1)

Here, we write down

$$G(s) = 1 - \{1 - G(s)\} \tag{B-2}$$

If we insert (B-2) into (B-1), then we obtain

$$A(s,x) = \int_{1+x}^{\infty} \frac{(z-x-1)dz}{z^2(z-1)^2} - \int_{1+x}^{\infty} \frac{(z-x-1)[1-G(sz)]dz}{z^2(z-1)^2}$$
 (B-3)

The first term of the right side (B-3) represents the term without LPM effect, the second term in (B-3) describes the influence of the LPM effect. At G(sz) = 1 the second term vanishes. Therefore, we could rewrite the (B-1) in the following way:

$$A(s,x) = A(BH) + A(LPM), (B-4)$$

where

$$A(BH) = \int_{1+x}^{\infty} \frac{(z-x-1)dz}{z^2(z-1)^2},$$
 (B-5)

$$A(LPM) = -\int_{1+x}^{\infty} \frac{(z-x-1)[1-G(sz)]dz}{z^2(z-1)^2}$$
 (B-6)

As (1 - G(sz)) in (B-6) is a non-negative monotonically decreasing function, A(LPM) is a non-positive function, which decreases the cross section as the logical consequence of the LPM effect. If the absolute value of the A(LPM) is negligible compared to A(BH), then, it is equivalent to the neglect of the LPM effect.

Now, let us examine the degree of the LPM effect, calculating the A(s,x), B(s,x), C(s,x), D(s,x), E(s,x) for $E_{\mu}=10^{24}~eV$ in the lead. Thus, as the LPM effect is the strongest in the lead among four kinds of materials under consideration, it is enough to consider the case of the lead.

In Table B-1 we give A(BH), A(LPM) - E(BH), E(LPM). As it is clearly seen from the Table B-1, all the functions A(LPM) - E(LPM) are completely negligible for A(BH) - E(BH), respectively over all v and ρ . This is the reason why we assert that the LPM effect could be completely negligible for the direct pair production process up to 10^{24} eV.

In Table B-1, we give numerical values of A(BH), A(LPM) for different v and ρ in the case of lead with $10^{24}eV$. As you understand from these numerical values, the LPM effect could be completely negligible even in the lead with $10^{24}eV$.

References

- [1] Landau, L.D. and Pomeranchuk, I.J., Dokl. Akad. Nauk. SSSR (1953) 92, 535; 92,735
- [2] Migdal, A.B. Phys. Rev. (1956), 103, 1811
 Migdal, A.B. Zh. Eksp. Teor. Fiz., (1957), 32,633 (Sov. Phys. JETP 5,527)
- [3] Fowler, P.H. et al Phil. Mag. (1959) 4,1030
- [4] Varfolomeev, R.R. et al, Zh. Eksp. Teor. Fiz(1960), 38, 33 (Sov. Phys. JETP(1960)11, 23)
 Varfolomeev, R.R. et al Zh. Eksp. Ter. Fiz. (1976), 69, 429 (Sov. Phys. JETP (1976)42, 218)
- [5] M.L.Perl In Proc. 1994 Les Rencontres de Physique de la Valle D'Aoste (Editions Frontieres. Gifsur-Yvette, France, 1994) Ed. M.Grego, p.567.
- [6] Anthony, P et al Phys.Rev.Lett. (1995), 75, 1945
- [7] Anthony, P et al Phys.Rev.Lett. (1995), 76, 3550
- [8] Anthony, P et al. Phys..Rev.D(1997),56,1373
- [9] Misaki, A Phys.Rev.D (1989), 40,3086
 Misaki, A Fortschr.Phys. (1990),34,413
 Misaki, A Il Nuovo Cimento (1990),13,733
- [10] Konishi et al J.Phys.G (1991),17,719
- [11] L.A.Kuzmichev et al. Proceeding of the 26th ICRC Ed. by D.Kieda, M.Salomon & B.Dingus, Salt Lake Sity, Utah, 1999, vol.2 p.217
 I.A.Belolaptikov et al. Astroparticle Physics 7 (1997) 263
 V.A.Balkanov et al. Proc. 25th ICRC 7, (Durban,1997) 25
 I.A.Belolaptikov et al. Proc. 25th ICRC 7, (Durban,1997) 173
- [12] Hundertmark St. (for the AMANDA Collaboration). Proc. of the 26th ICRC, Salt Lake City, Utah. 1999. V.2. pp.12-15.
 Andres E. Askebjer P., Barwick S.W. et al. (AMANDA Collaboration) The AMANDA neutrino telescope: principle of operation and first results astro-ph/9906203.
 Spiering Ch. (for the AMANDA Collaboration) AMANDA: status, results and fiture astro-ph/9906205.
 AMANDA Collaboration, Proc. 7th Int. Workshop on Neutrino Telescopes, Venice 1996
 P. Askebjer et al. Nuclear Physics B (Proc. Suppl.) 52B (1997), 256
- [13] M.L.Ter-Mikaelian, Dokl.Akad.Nauk.SSSR 94,1033 (1954).
- [14] S.Polityko, N.Takahashi, M.Kato and A.Misaki, Proc. RIKEN International Workshop on Electromagnetic and Nuclear Cascade Phenomena in High and Extremely High Energies, Japan, 414 (1994).
- [15] V.N.Baier, V.M.Katkov and V.S.Fadin, Radiation of Relativistic Electrons. Atomizdat. Moscow. 1973.
- [16] V.B. Berestetskii, E.M. Lifshitz and L.P. Pitaevskii, Quantum electrodynamics, Pergamon Press, Oxford (1982).
- [17] W.Lohman, R.Koop and R.Voss, CERN 85-03, (1985).
- [18] R.P.Kokoulin and A.A.Petruchin, in Proc. of the 11th International Conference on Cosmic Rays, Budapest, Hungary, (1969), ed.by T.Gemesy et al. (Akademiai Kiado, Budapest, 1970), vol.4, 277
- [19] A.A.Petruchin and V.V.Shestakov, Can.J.Phys. (1968), 46,377.
- [20] E.V.Bugaev, V.A.Naumov, S.I.Sinegovsky, A.Misaki, N.Takahashi and E.S.Zaslavskaya Preprint DFF 204/4/1994 Page 18-19 Dipartimento di Fisica and Istituto Nationale di Fisica Nucleare, Sezione di Firenze

- [21] V.N.Baier, V.M.Katkov Phys.Rev **D** 57,3146 (1998).
- [22] F.F.Ternovskii Sov.Phys.JETP, v.37(10), no.4,718, (1960).
- [23] Sakumoto et al. Phys.Rev. D v.49.no 9. 1992. p. 3042.
- [24] A.Misaki et al. Proceeding of the 26^{th} ICRC Ed. by D.Kieda, M.Salomon & B.Dingus, Salt Lake Sity, Utah, 1999, vol.2 pp.139-142.

- Figure 1 Differential cross sections for bremsstrahlung processes in water. LPM denotes the case with the LPM effect and LPM+LD denotes the case with longitudinal effect (LD) in addition to the LPM effect, while BH denotes the case without the LPM effect (the Bethe-Heitler case) and BH+LPM effect denotes the case without the LPM effect and with the LD effect. [a] denotes 10¹⁵eV, the primary energy of the muon and [b] to [ji] denote 10¹⁶ to 10²⁴eV, primary energy of the muons, respectively.
- **Figure 2** Differential cross sections for bremsstrahlung processes in standard rock. The notations in the figure are the same as in Figure 1
- **Figure 3** Differential cross sections for bremsstrahlung processes in iron. The notations in the figure are the same as in Figure 1.
- **Figure 4** Differential cross sections for bremsstrahlung processes in lead The notations in the figure are the same as in Figure 1.
- **Figure 5** Ratio of the total cross sections σ_{BH+LD} to σ_{BH} for various materials.
- Figure 6 Ratio of the total cross sections σ_{LPM+LD} to σ_{LPM} for various materials.
- **Figure 7** Mean free paths for bremsstrahlung processes in water The notations in the figure are the same as in Figure 1.
- **Figure 8** Mean free paths for bremsstrahlung processes in standard rock The notations in the figure are the same as in Figure 1.
- **Figure 9** Mean free paths for bremsstrahlung processes in iron. The notations in the figure are the same as in Figure 1.
- **Figure 10** Mean free paths for bremsstrahlung processes in lead. The notations in the figure are the same as in Figure 1.
- Figure 11 Mean free paths for bremsstrahlung processes with the LPM effect for various materials.
- Figure 12 Mean free paths for the bremsstrahlung process with the LPM and the LD effect for various materials.
- Figure 13-1 Differential virtual gamma rays energy spectrum for direct electron pair production processes for the primary energy with $10^{16} eV$
- Figure 13-2 Differential virtual gamma rays energy spectrum for direct electron pair production processes for the primary energy with $10^{24} eV$.
- Figure 14 Total cross sections for direct electron pair production process for various materials
- Figure 15 Mean free paths for direct electron pair production process for various materials.
- Figure 16-1 Effective energy loss for bremsstrahlung process due to both with and without LPM effect for the iron and water.
- Figure 16-2 Effective energy loss for bremsstrahlung process due to both with and without LPM effect for the lead and s.r.
- Figure 17 The Ratio of the effective energy loss with the LPM effect to without the LPM effect for bremsstrahlung process for various materials
- Figure 18 Effective energy loss for direct electron pair production process for various materials.

- Figure 19-1 Decrease of average energy of muon in the standard rock Ordinate axis means average energy of muon divided the sampling number of muons for both the cases with and without the LPM effect. LPM 24-21 means primary energy of muon with $10^{24}eV$ and the cut off energy of muon with $10^{21}eV$ with the LPM effect, while BH 24-21 correspond to the case without the LPM effect (Bethe-Heitler case). LPM 23-29 means primary energy of muon with $10^{23}eV$ and the cut off energy of muon with $10^{23}eV$ with the LPM effect , while BH 23-20- means the primary energy of muon and the cut off energy of muon with $10^{20}eV$ without the LPM effect .
- Figure 19-2 Decrease of average energy of muon in water. The date correspond to those in Figure 19-1.
- Figure 20-1 Survival probability of muon in standard rock LPM 24-21 and other notations are the same as in Figure 19-1.
- Figure 20-2 Survival probability of muon in water. The date correspond to those in Figure 19-1.
- Figure 21-1 Range distribution of muon in standard rock LPM 24-21 and other notations are the same as in Figure 19-1
- **Figure 21-2** Range distribution of muon in water. Notations in the figure are the same as in Figure 19-1. The area covered with the range distribution is normalized to unity.
- **Figure 22-1** Differential energy spectrum in water: LPM 22-19 and BH 22-19 are of the same meaning as in Figure 19-1.
- **Figure 22-2** Differential energy spectrum in water: LPM 23-20 and BH 23-20 are of the same meaning as in Figure 19-1.
- Figure 22-3 Differential energy spectrum in water: LPM 24-21 and BH 24-21 are of the same meaning as in Figure 19-1.
- Figure 23-1 Differential energy spectrum in standard rock: LPM 22-19 and BH 22-19 are of the same meaning as in Figure 19-1.
- **Figure 23-2** Differential energy spectrum in standard rock: LPM 23-20 and BH 23-20 are of the same meaning as in Figure 19-1.
- Figure 23-3 Differential energy spectrum in standard rock: LPM 24-21 and BH 24-21 are of the same meaning as in Figure 19-1.
- Table 1 Some parameters for the bremsstrahlung process
- **Table 2** Some parameters for the direct electron pair production process
- **Table 3** Mean values and their standard deviations of range fluctuation of muons in water.
- Table 4 Mean values and their standard deviations of range fluctuation of muons in standard rock.
- **Table B-1** A(BH) and A(LPM) in the Ternovskii functions.

Table 1:

	Water (H_2O)	St.rock	Lead (Pb)	Fe
Z	7.23	11	82	26
A	14.3	22	207.2	55.85
$\rho(g \cdot cm^{-3})$	1.0	2.65	11.34	7.86
$n(cm^{-3})$	$4.211 \cdot 10^{22}$	$7.254 \cdot 10^{22}$	$3.296 \cdot 10^{22}$	$8.475 \cdot 10^{22}$
L	8.85	8.57	7.23	7.99
$E_{LPM}(eV)$	$2.49 \cdot 10^{24}$	$6.44 \cdot 10^{23}$	$3.02 \cdot 10^{22}$	$1.06 \cdot 10^{23}$
$\omega_0(eV)$	20.49	33.18	61.06	55.14

Table 2:

	Water (H_2O)	St.rock	Lead (Pb)	Iron (Fe)
L	5.76	5.62	4.95	5.33
$E_{LPM}(eV)$	$3.84 \cdot 10^{24}$	$0.98 \cdot 10^{24}$	$4.41 \cdot 10^{22}$	$1.59 \cdot 10^{23}$

Table 3:

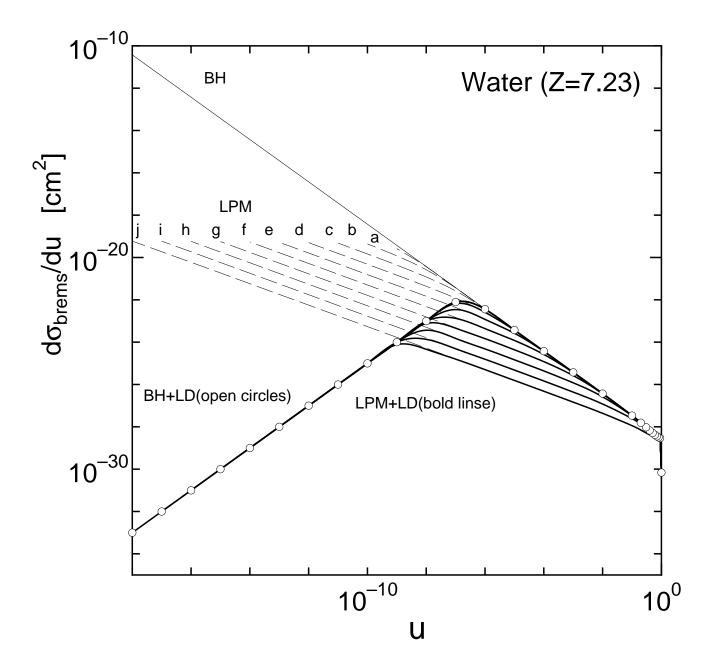
Muon energy		ВН		LPM	
$E_{prim}[eV]$	$E_{cut}[eV]$	$\langle R \rangle$	σ	$\langle R \rangle$	σ
10^{24}	10^{21}	34.28	14.60	38.44	16.93
10^{23}	10^{20}	32.71	14.53	33.79	15.00
10^{22}	10^{19}	33.85	14.97	33.95	15.04
10^{21}	10^{18}	35.00	15.39	34.99	15.42
10^{20}	10^{17}	36.09	15.77	36.07	15.80

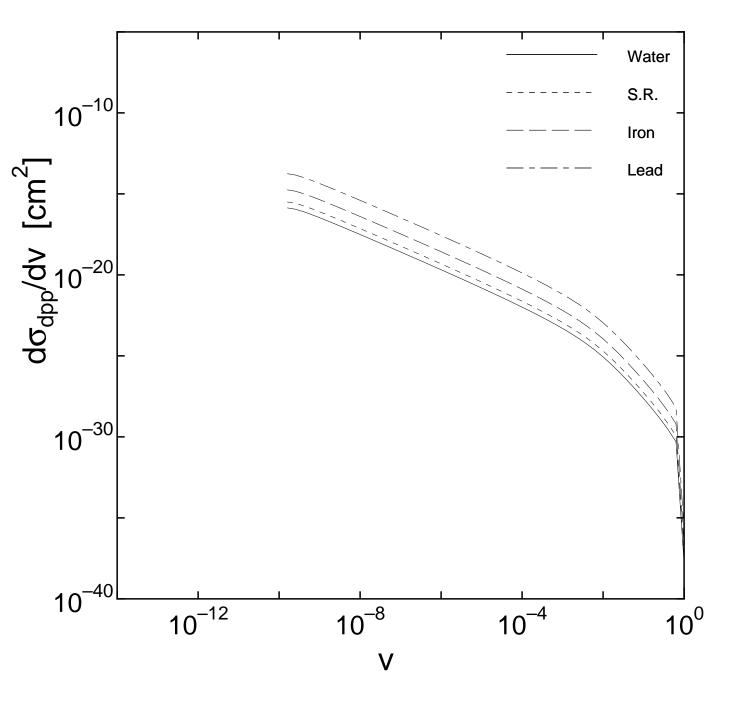
Table 4:

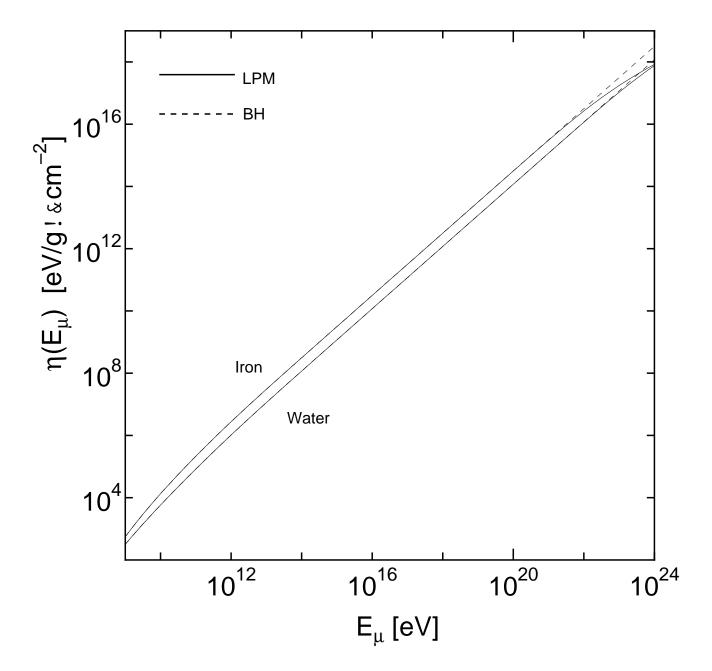
Muon energy		ВН		LPM	
$E_{prim}[eV]$	$E_{cut}[eV]$	$\langle R \rangle$	σ	$\langle R \rangle$	σ
10^{24}	10^{21}	26.36	11.23	35.30	15.82
10^{23}	10^{20}	25.15	11.17	27.32	12.09
10^{22}	10^{19}	26.03	11.51	26.31	11.66
10^{21}	10^{18}	26.91	11.84	26.91	11.86
10^{20}	10^{17}	27.75	12.13	27.74	12.15

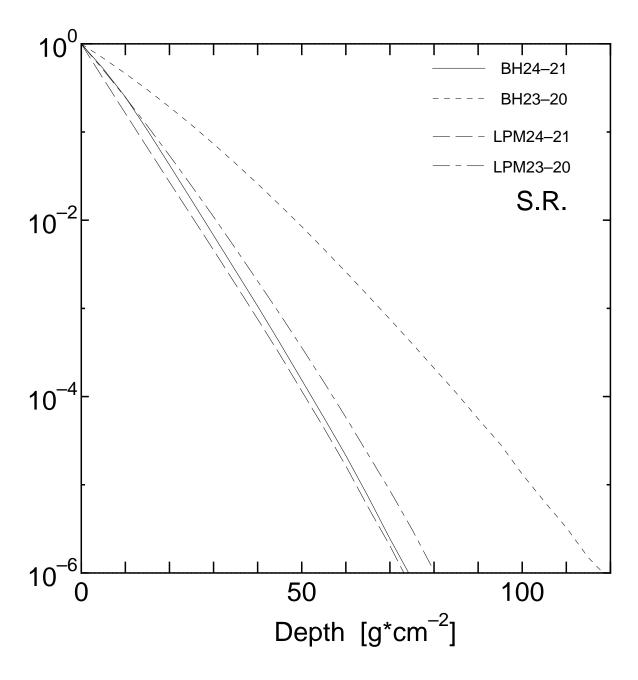
Table 5:

v	ρ	A (BH)	A (LPM)
$1.022 \cdot 10^{-18}$	$0.000 \cdot 10^{0}$	$7.157263 \cdot 10$	$0.000000 \cdot 10^{0}$
$1.000 \cdot 10^{-17}$	$0.000 \cdot 10^{0}$	$6.701101 \cdot 10$	$0.000000 \cdot 10^{0}$
$1.000 \cdot 10^{-17}$	$5.000 \cdot 10^{-1}$	$6.729869 \cdot 10$	$0.000000 \cdot 10^{0}$
$1.000 \cdot 10^{-17}$	$9.475 \cdot 10^{-1}$	$6.929182 \cdot 10$	$0.000000 \cdot 10^{0}$
$1.000 \cdot 10^{-16}$	$0.000 \cdot 10^{0}$	$6.240584 \cdot 10$	$0.000000 \cdot 10^{0}$
$1.000 \cdot 10^{-16}$	$5.000 \cdot 10^{-1}$	$6.269352 \cdot 10$	$0.000000 \cdot 10^{0}$
$1.000 \cdot 10^{-16}$	$9.949 \cdot 10^{-1}$	$6.698923 \cdot 10$	$0.000000 \cdot 10^{0}$
$1.000 \cdot 10^{-15}$	$0.000 \cdot 10^{0}$	$5.780067 \cdot 10$	$0.000000 \cdot 10^{0}$
$1.000 \cdot 10^{-15}$	$5.000 \cdot 10^{-1}$	$5.808835 \cdot 10$	$0.000000 \cdot 10^{0}$
$1.000 \cdot 10^{-15}$	$9.995 \cdot 10^{-1}$	$6.468665 \cdot 10$	$0.000000 \cdot 10^{0}$
$1.000 \cdot 10^{-14}$	$0.000 \cdot 10^{0}$	$5.319550 \cdot 10$	$0.000000 \cdot 10^{0}$
$1.000 \cdot 10^{-14}$	$5.000 \cdot 10^{-1}$	$5.348318 \cdot 10$	$0.000000 \cdot 10^{0}$
$1.000 \cdot 10^{-14}$	$9.999 \cdot 10^{-1}$	$6.238406 \cdot 10$	$0.000000 \cdot 10^{0}$ $0.000000 \cdot 10^{0}$
$1.000 \cdot 10^{-13}$	$0.000 \cdot 10^{0}$	$4.859033 \cdot 10$	$0.000000 \cdot 10^{0}$ $0.000000 \cdot 10^{0}$
$1.000 \cdot 10$ $1.000 \cdot 10^{-13}$	$5.000 \cdot 10^{-1}$	$4.887801 \cdot 10$	$0.000000 \cdot 10^{0}$ $0.000000 \cdot 10^{0}$
$1.000 \cdot 10$ $1.000 \cdot 10^{-13}$			
$1.000 \cdot 10^{-13}$ $1.000 \cdot 10^{-12}$	$1.000 \cdot 10^{0}$	$6.008148 \cdot 10$	$0.000000 \cdot 10^{0}$
$1.000 \cdot 10^{-12}$ $1.000 \cdot 10^{-12}$	$0.000 \cdot 10^{0}$	$4.398515 \cdot 10$	$0.000000 \cdot 10^{0}$
	$5.000 \cdot 10^{-1}$	$4.427284 \cdot 10$	$0.000000 \cdot 10^{0}$
$1.000 \cdot 10^{-12}$	$1.000 \cdot 10^{0}$	$5.777889 \cdot 10$	$0.000000 \cdot 10^{0}$
$1.000 \cdot 10^{-11}$	$0.000 \cdot 10^{0}$	$3.937998 \cdot 10$	$0.000000 \cdot 10^{0}$
$1.000 \cdot 10^{-11}$	$5.000 \cdot 10^{-1}$	$3.966767 \cdot 10$	$0.000000 \cdot 10^{0}$
$1.000 \cdot 10^{-11}$	$1.000 \cdot 10^{0}$	$5.547631 \cdot 10$	$0.000000 \cdot 10^{0}$
$1.000 \cdot 10^{-10}$	$0.000 \cdot 10^{0}$	$3.477481 \cdot 10$	$0.000000 \cdot 10^{0}$
$1.000 \cdot 10^{-10}$	$5.000 \cdot 10^{-1}$	$3.506250 \cdot 10$	$0.000000 \cdot 10^{0}$
$1.000 \cdot 10^{-10}$	$1.000 \cdot 10^{0}$	$5.317372 \cdot 10$	$0.000000 \cdot 10^{0}$
$1.000 \cdot 10^{-9}$	$0.000 \cdot 10^{0}$	$3.016964 \cdot 10$	$0.000000 \cdot 10^{0}$
$1.000 \cdot 10^{-9}$	$5.000 \cdot 10^{-1}$	$3.045733 \cdot 10$	$0.000000 \cdot 10^{0}$
$1.000 \cdot 10^{-9}$	$1.000 \cdot 10^{0}$	$5.087114 \cdot 10$	$0.000000 \cdot 10^{0}$
$1.000 \cdot 10^{-8}$	$0.000 \cdot 10^{0}$	$2.556447 \cdot 10$	$0.000000 \cdot 10^{0}$
$1.000 \cdot 10^{-8}$	$5.000 \cdot 10^{-1}$	$2.585216 \cdot 10$	$0.000000 \cdot 10^{0}$
$1.000 \cdot 10^{-8}$	$1.000 \cdot 10^{0}$	$4.856855 \cdot 10$	$0.000000 \cdot 10^{0}$
$1.000 \cdot 10^{-7}$	$0.000 \cdot 10^{0}$	$2.095930 \cdot 10$	$0.000000 \cdot 10^{0}$
$1.000 \cdot 10^{-7}$	$5.000 \cdot 10^{-1}$	$2.124699 \cdot 10$	$0.000000 \cdot 10^{0}$
$1.000 \cdot 10^{-7}$	$1.000 \cdot 10^{0}$	$4.626597 \cdot 10$	$0.000000 \cdot 10^{0}$
$1.000 \cdot 10^{-6}$	$0.000 \cdot 10^{0}$	$1.635413 \cdot 10$	$0.000000 \cdot 10^{0}$
$1.000 \cdot 10^{-6}$	$5.000 \cdot 10^{-1}$	$1.664182 \cdot 10$	$0.000000 \cdot 10^{0}$
$1.000 \cdot 10^{-6}$	$1.000 \cdot 10^{0}$	$4.396338 \cdot 10$	$0.000000 \cdot 10^{0}$
$1.000 \cdot 10^{-5}$	$0.000 \cdot 10^{0}$	$1.174898 \cdot 10$	$-3.030322 \cdot 10^{-6}$
$1.000 \cdot 10^{-5}$	$5.000 \cdot 10^{-1}$	$1.203666 \cdot 10$	$-1.751002 \cdot 10^{-6}$
$1.000 \cdot 10^{-5}$	$1.000 \cdot 10^{0}$	$4.166079 \cdot 10$	$0.000000 \cdot 10^{0}$
$1.000 \cdot 10^{-4}$	$0.000 \cdot 10^{0}$	$7.145755 \cdot 10^{0}$	$-1.698723 \cdot 10^{-4}$
$1.000 \cdot 10^{-4}$	$5.000 \cdot 10^{-1}$	$7.432968 \cdot 10^{0}$	$-1.002189 \cdot 10^{-4}$
$1.000 \cdot 10^{-4}$	$1.000 \cdot 10^{0}$	$3.935811\cdot 10$	$0.000000 \cdot 10^0$
$1.000 \cdot 10^3$	$0.000 \cdot 10^{0}$	$2.645587 \cdot 10^{0}$	$-4.427908 \cdot 10^3$
$1.000 \cdot 10^3$	$5.000 \cdot 10^{-1}$	$2.910863 \cdot 10^{0}$	$-2.918965 \cdot 10^3$
$1.000 \cdot 10^{3}$	$1.000 \cdot 10^{0}$	$3.705456\cdot 10$	$0.000000 \cdot 10^{0}$
$1.000 \cdot 10^2$	$0.000 \cdot 10^{0}$	$7.112332 \cdot 10^2$	$-2.047297 \cdot 10^{-4}$
$1.000 \cdot 10^2$	$5.000 \cdot 10^{-1}$	$1.066582 \cdot 10^{-1}$	$-3.217814 \cdot 10^{-4}$
$1.000 \cdot 10^2$	$1.000 \cdot 10^{0}$	$3.474261 \cdot 10$	$0.000000 \cdot 10^{0}$
$1.000 \cdot 10^{-1}$	$0.000 \cdot 10^{0}$	$1.171890 \cdot 10^{-5}$	$-2.204098 \cdot 10^{-13}$
$1.000 \cdot 10^{-1}$	$5.000 \cdot 10^{-1}$	$2.077567 \cdot 10^{-5}$	$-7.148156 \cdot 10^{-13}$
$1.000 \cdot 10^{-1}$	$1.000 \cdot 10^{0}$	$3.233732 \cdot 10$	$0.000000 \cdot 10^{0}$
$1.000 \cdot 10^{0}$	$0.000 \cdot 10^{0}$	$0.000000 \cdot 10^{0}$	$0.000000 \cdot 10^{0}$
$1.000 \cdot 10^{0}$	$5.000 \cdot 10^{-1}$	$0.000000 \cdot 10^{0}$	$0.000000 \cdot 10^{0}$
$1.000 \cdot 10^{0}$	$1.000 \cdot 10^{0}$	$2.363193 \cdot 10^{-10}$	$0.000000 \cdot 10^{0}$
1.000 10	1.000 10	2.000100 10	0.00000 10

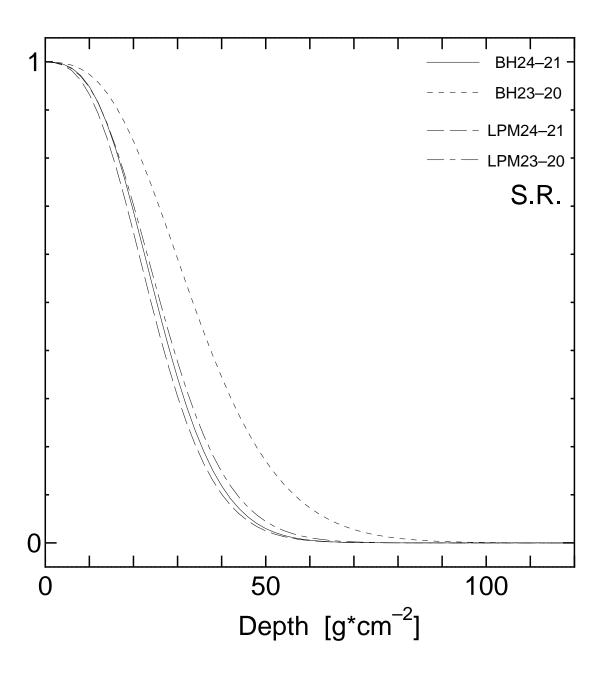




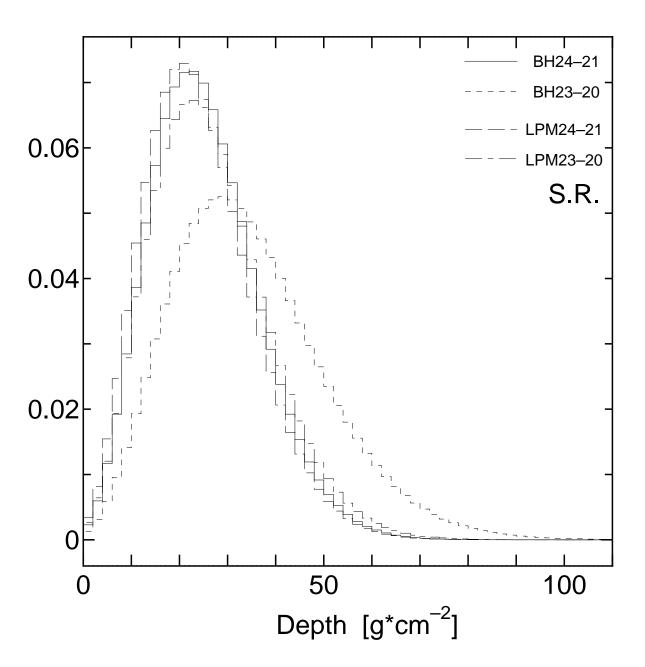




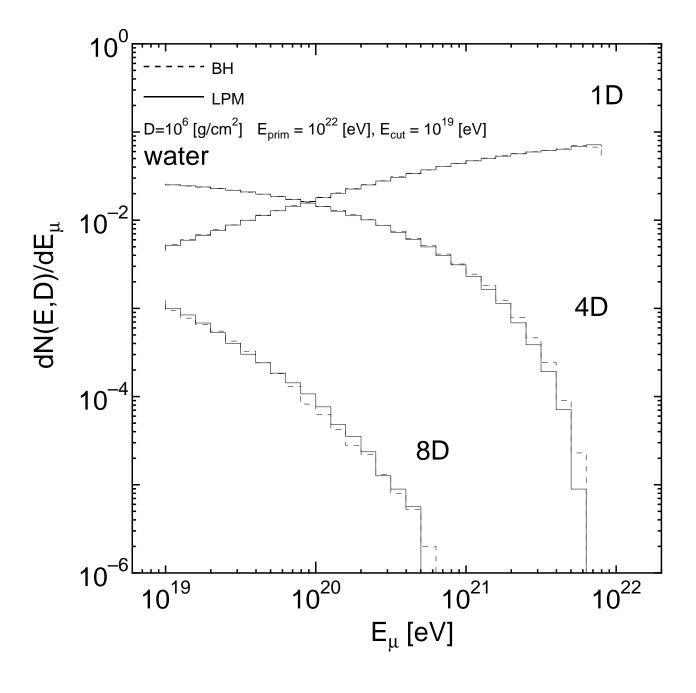
[×10⁺⁵]

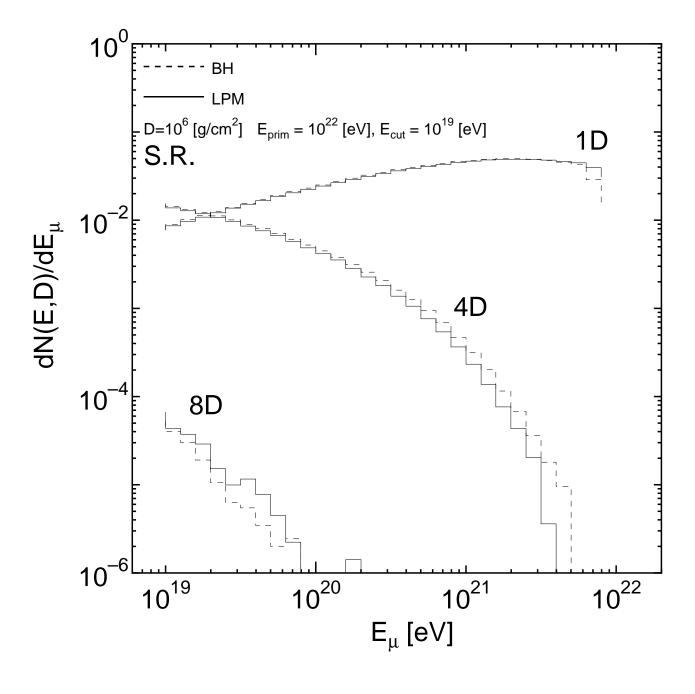


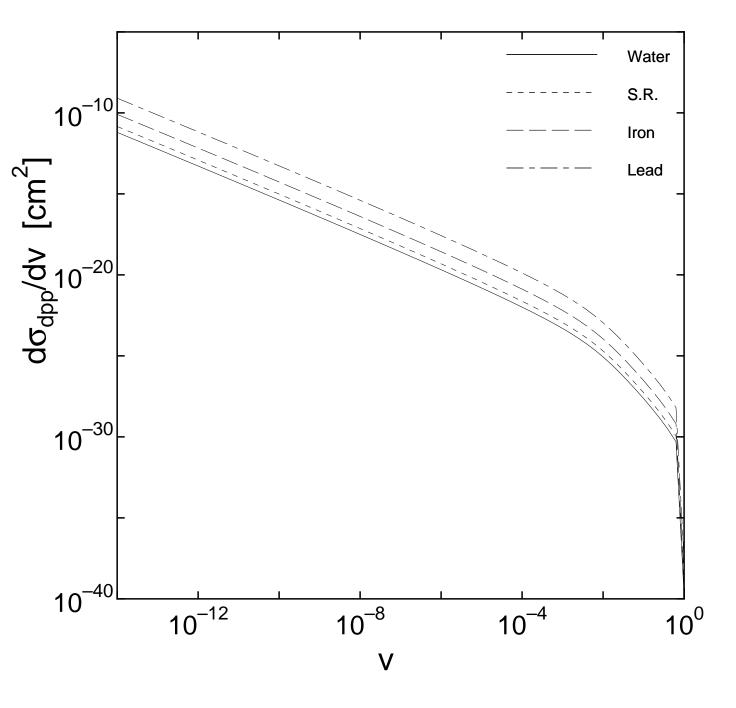
[×10⁺⁵]

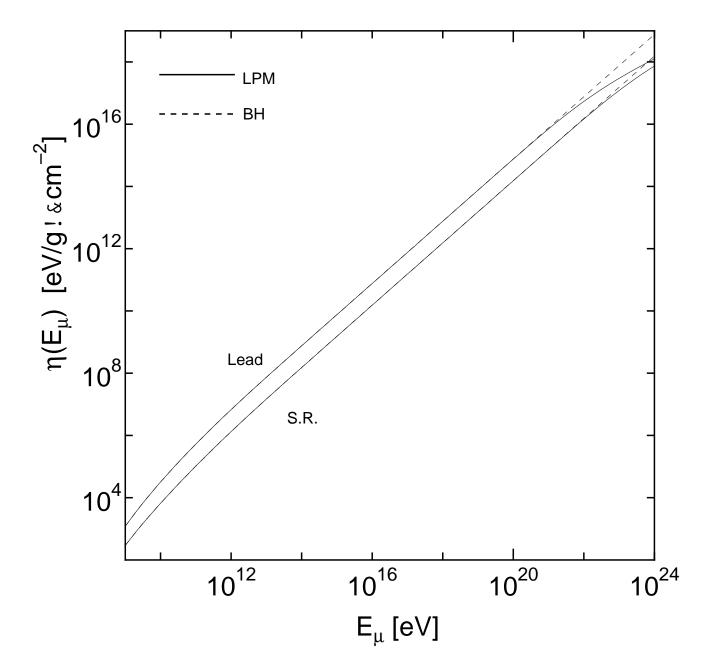


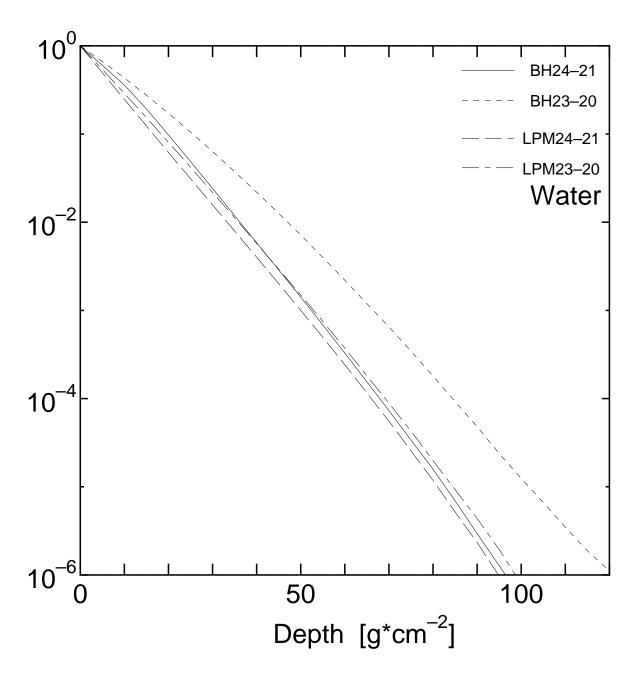
[×10⁺⁵]



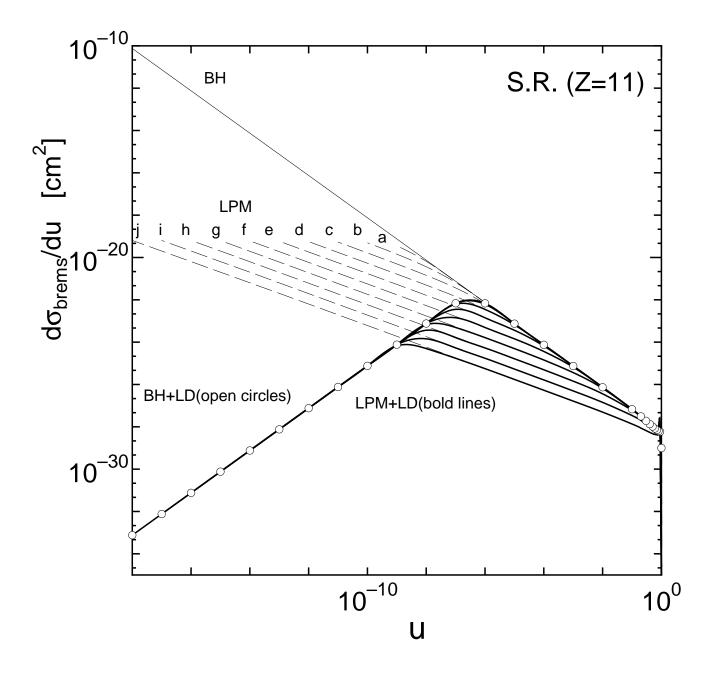


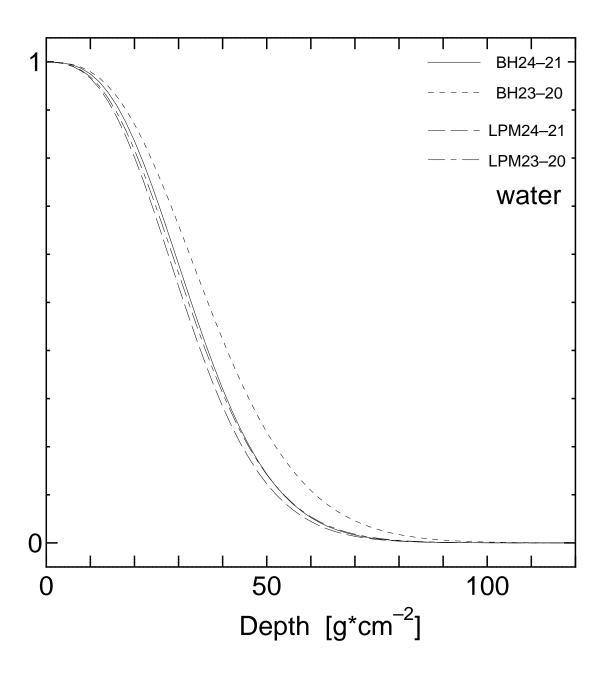




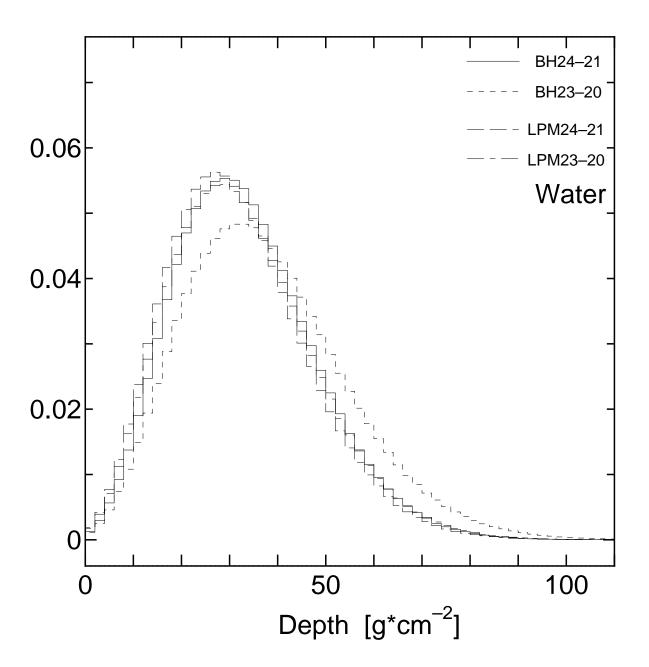


[×10⁺⁵]





[×10⁺⁵]



[×10⁺⁵]

